



Experimental Observations of Strange Non-Chaotic Attractors from a Chaotic Neuron Integrated Circuit

Seiji Uenohara[†], Yoshihiko Horio[†], Takahito Mitsui^{‡,*} and Kazuyuki Aihara^{‡,*}

[†]Graduate School of Engineering, Tokyo Denki University, 2-2 Kanda-Nishiki-cho, Chiyoda-ku, Tokyo 101-8457, Japan

* FIRST, Aihara Innovative Mathematical Modelling Project, JST, 4-6-1 Komaba, Meguro-ku, Tokyo 153-8505, Japan

[‡]Institute of Industrial Science, The University of Tokyo, 4-6-1 Komaba, Meguro-ku, Tokyo 153-8505, Japan

E-mail: uenohara-seiji@edu.brain.kyutech.ac.jp, horio@eee.dendai.ac.jp, mitsui@sat.t.u-tokyo.ac.jp

Abstract—Strange non-chaotic attractors are observed experimentally in a chaotic neuron integrated circuit that implements a chaotic neuron model driven by an external quasiperiodic signal. Lyapunov and phase sensitivity exponents are used to classify the observed attractors into the following three types: 1) chaotic attractors; 2) tori; and 3) strange non-chaotic attractors. In experiments, it is generally difficult to extract precise values for the non-positive largest Lyapunov exponents from the resulting time series. Therefore, a mathematical model of the circuit is constructed, such that the attractors obtained from the experimental behavior can be reproduced accurately in simulations. By analyzing the mathematical model instead of directly analyzing the time series from the circuit, the observed attractors are successfully characterized, including SNAs.

1. Introduction

Strange non-chaotic attractors (SNAs), with fractal structure and a non-positive Lyapunov exponent, appear in the responses largest of nonlinear systems to quasiperiodically varying external forces [1]. So far, SNAs have been observed both numerically in various nonlinear models [2, 3] and experimentally, for example, in electrical circuits [4, 5]. (See also [6] for review and references therein).

In this paper, SNAs are observed in experiments conducted with a chaotic neuron integrated circuit that implements a chaotic neuron model [7]. Lyapunov and phase sensitivity exponents are used to classify the observed attractors into the following three types: 1) chaotic attractors with a positive Lyapunov exponent; 2) tori with non-positive Lyapunov exponents and zero phase sensitivity exponent; and 3) strange non-chaotic attractors with a non-positive Lyapunov exponents and a non-zero phase sensitivity exponent. It is seen that the non-positive largest Lyapunov exponent is important in distinguishing SNAs from chaotic attractors. However, it is difficult to calculate a precise value for the non-positive largest Lyapunov exponent from the time series obtained from experiments employing the circuit.

Therefore, a mathematical model of the circuit, which can reproduce the attractors seen in the experimental output, is constructed. This model is then used to evaluate

the experimentally observed attractors; toward this end, a chaotic neuron model with a quasiperiodic force, which can reproduce all the type of attractors, is introduced in Section 2.

In Section 3, methods for calculating the Lyapunov exponents, and the phase sensitivity exponent, are explained. In Section 4, the results from the circuit experiments can be evaluated by using values of the characteristic exponents calculated through the mathematical model. Thus, the attractors obtained from the circuit are classified.

2. Chaotic neuron model with a quasiperiodic external force

A chaotic neuron model [7] with a quasiperiodic external force can be expressed as

$$y(t+1) = k_r y(t) + \alpha f(h(t)) + a, \quad (1)$$

$$h(t+1) = y(t+1) + b \cos(2\pi\theta(t+1)), \quad (2)$$

$$\theta(t+1) = \theta(t) + \omega \bmod 1, \quad (3)$$

where t is the discrete-time variable, $y(t)$ is the internal state of the neuron, k_r is the decay coefficient of the internal state, α is a scaling parameter for the refractoriness, a is a bias on the system, and $f(\cdot)$ is a monotonically decreasing nonlinear function as described below. Moreover, $b \cos(2\pi\theta(t))$ is a quasiperiodic external force with amplitude b and phase $\theta(t)$, and $\omega = (\sqrt{5} - 1)/2$.

Part of the chaotic neuron integrated circuit used in the experiments is shown in Figure 1 [8]. In this figure, the nonlinear output function circuit for the neuron is enclosed by broken lines, and the input-output characteristic for this circuit can be controlled through external voltages, V_{FN} and V_{FP} .

As mentioned in Section 1, the characteristic exponents must be measured to classify the types of attractors. To calculate these exponents, a mathematical expression for the transfer characteristic of the output circuit, and its derivative, are necessary. However, explicitly describing the transfer characteristic of the nonlinear output function circuit is difficult because of complex physical phenomena resulting from the MOSFETs in the circuit. Therefore, cubic spline interpolation of the measured transfer curve, which is continuous and piecewise differentiable, is employed to

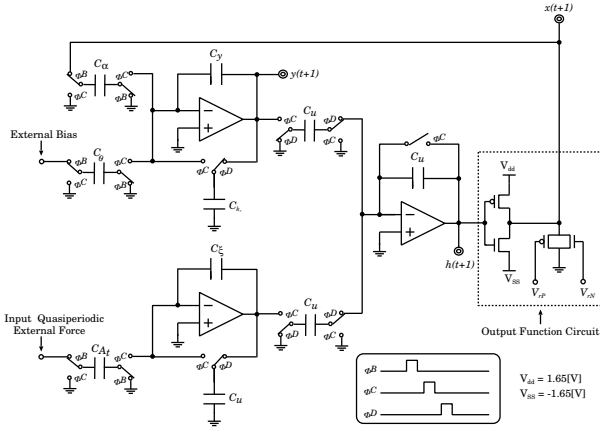


Figure 1: Schematic of part of the chaotic neuron integrated circuit [8]. ΦB , ΦC , and ΦD are non-overlapping clocks.

model the characteristic. The form of nonlinear output function $f(\cdot)$ is shown in Figure 2.

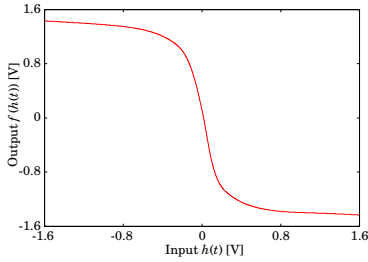


Figure 2: The form of nonlinear output function $f(\cdot)$.

3. Numerical characterization of attractors

The Lyapunov exponents, $\{\lambda_y, \lambda_\theta\}$ and the phase sensitivity exponent, μ , are used to categorize the obtained attractors. In this section, a précis of the methods used to calculate $\{\lambda_y, \lambda_\theta\}$ and μ [9] is given.

Without quasiperiodic external force, $b \cos(2\pi\theta(t))$, the chaotic neuron model is a one-dimensional discrete-time dynamical system with respect to the internal state, $y(t)$. By applying $b \cos(2\pi\theta(t))$, however, the chaotic neuron model becomes a two-dimensional discrete-time dynamical system. As a result, the orbital instability of the chaotic neuron circuit with $b \cos(2\pi\theta(t))$ included must be evaluated by using two Lyapunov exponents. However, one of Lyapunov exponent, say λ_θ , is always zero owing to the rigid rotation, Eq. (3).

Therefore, only the Lyapunov exponent with respect to the direction of $y(t)$, that is, λ_y , is considered, which can be obtained from

$$\lambda_y = \lim_{T \rightarrow \infty} \frac{1}{T} \sum_{t=0}^{T-1} \log \left| \frac{\partial y(t+1)}{\partial y(t)} \right|. \quad (4)$$

By defining the two partial derivatives of $h(t)$ in (2) with respect to $y(t)$ and $\theta(t)$ as $h_y(t)$ and $h_\theta(t)$, respectively, partial differentiation of $y(t+1)$ with respect to $\theta(t+1)$ leads to

$$\frac{\partial y(t+1)}{\partial \theta(t+1)} = h_\theta(t) + h_y(t) \frac{\partial y(t)}{\partial \theta(t)}. \quad (5)$$

In (5), the second term on the right-hand side contains $\partial y(t)/\partial \theta(t)$, which is equal to the term on the left-hand side at the previous time step. Hence, (5) can be rewritten as

$$\frac{\partial y(t+1)}{\partial \theta(t+1)} = \sum_{k=1}^{t+1} h_\theta(k-1) R_{t+1-k}(k) + R_{t+1}(0) \frac{\partial y(0)}{\partial \theta(0)}, \quad (6)$$

where

$$R_t(k) = \prod_{i=0}^{t-1} h_y(k+i), \quad (7)$$

and $R_t(0) = 1$. When $\lambda_y < 0$, the second term on the right-hand side of (6) decreases exponentially for large t , meaning that this term can be ignored.

Moreover, to find the exponent μ , suppose that

$$S_t = \sum_{k=1}^t h_\theta(k-1) R_{t-k}(k), \quad (8)$$

and

$$\gamma(t) = \max_{0 \leq t' \leq t} |S_{t'}|. \quad (9)$$

Then, the phase sensitivity function $\Gamma(t)$ is defined as the smallest value of $\gamma(t)$ for the initial conditions:

$$\Gamma(t) = \min_{y(0), \theta(0)} \gamma(t). \quad (10)$$

In general, the phase sensitivity function $\Gamma(t)$ is bounded for smooth attractors for large t . In contrast, for SNAs, which are non-smooth, $\Gamma(t)$ grows with t as

$$\Gamma(t) \simeq t^\mu, \quad (11)$$

where $\mu > 0$ is the phase sensitivity exponent. In this paper, the measured attractors are classified into three categories according to λ_y and μ : 1) chaotic attractors with $\lambda_y > 0$; 2) tori with $\lambda_y < 0$ and $\mu = 0$; and 3) SNAs with $\lambda_y < 0$ and $\mu > 0$.

4. Experimental results

When conducting the experiments using the circuit in Figure 1, the amplitude b of the external quasiperiodic force was changed and $y(t)$ and $\theta(t)$ were observed, for two different sets (Case 1 and Case 2) of the parameters a , k_r , α , V_{rN} , and V_{rP} . For Case 1, $\alpha = 0.646$, $k_r = 0.835$, $a = -0.338$, $V_{rN} = 1.6$ V, and $V_{rP} = -1.6$ V. For Case 2, $\alpha = 0.646$, $k_r = 0.835$, $a = -0.208$, $V_{rN} = 1.3$ V, and $V_{rP} = -1.3$ V.

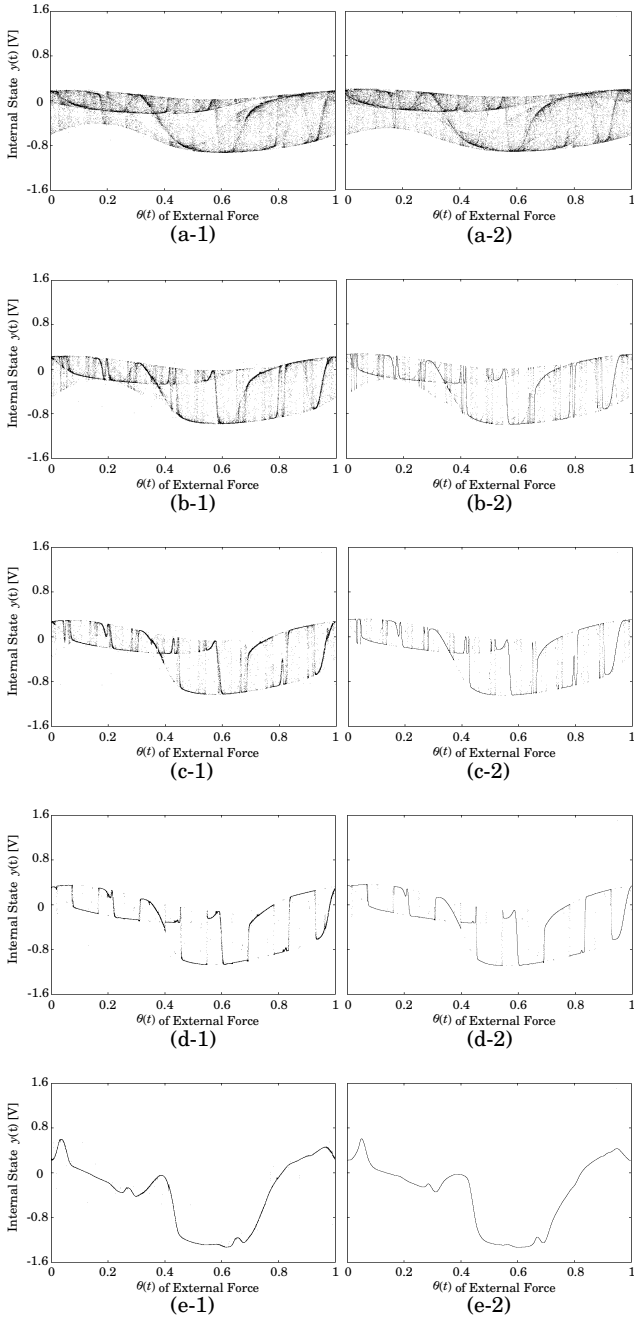


Figure 3: (Left panels) Experimental results for Case 1 with (a-1) $b = 0.04$, (b-1) $b = 0.06$, (c-1) $b = 0.08$, (d-1) $b = 0.1$, and (e-1) $b = 0.16$. (Right panels) Numerical results from the corresponding mathematical model for (a-2) $\lambda_y = 0.166$, (b-2) $\lambda_y = -0.418$, (c-2) $\lambda_y = -0.484$, (d-2) $\lambda_y = -0.66$, and (e-2) $\lambda_y = -0.481$.

The experimental results and their simulated counterparts are shown in Figures 3 and 4, respectively. Figure 5 then shows time evolutions of the phase sensitivity function $\Gamma(t)$ for nonchaotic attractors in the right-hand panels of Figures 3 and 4.

From the results for Case 1 shown in Figure 3, in (a-2)

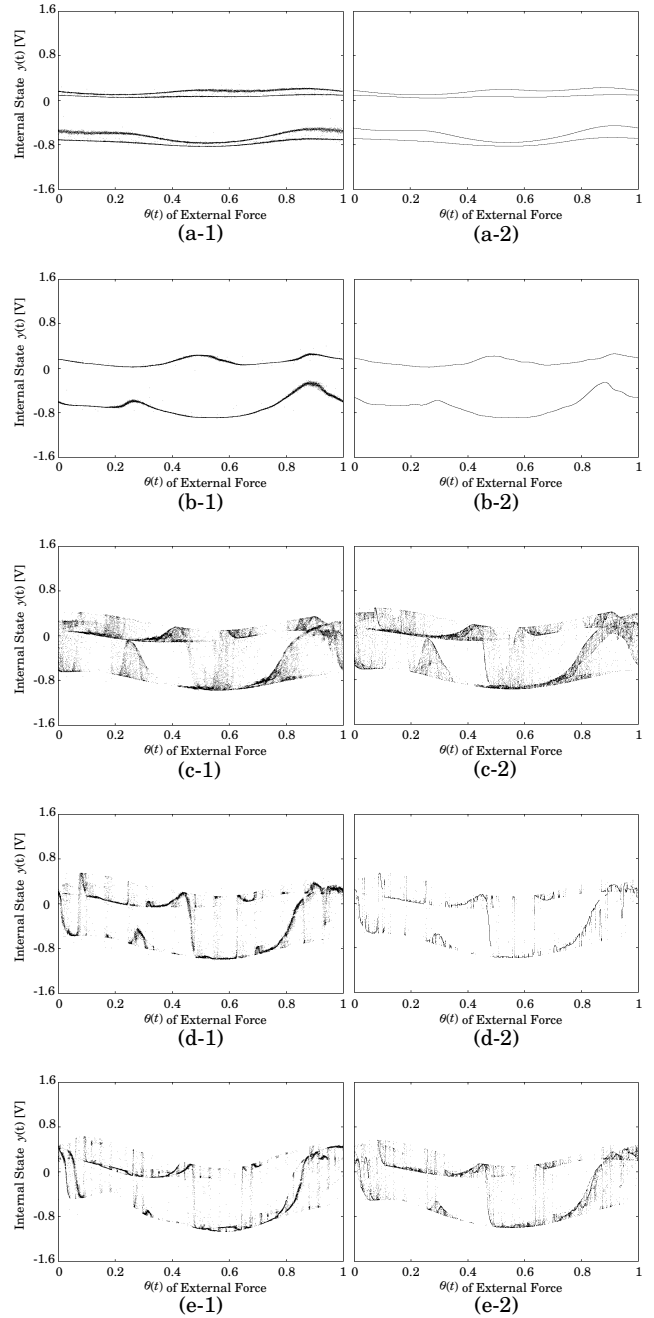


Figure 4: (Left panels) Experimental results for Case 2 with (a-1) $b = 0.04$, (b-1) $b = 0.08$, (c-1) $b = 0.1$, (d-1) $b = 0.12$, and (e-1) $b = 0.14$. (Right panels) Numerical results from the corresponding mathematical model for (a-2) $\lambda_y = -0.19$, (b-2) $\lambda_y = -0.206$, (c-2) $\lambda_y = 0.1$, (d-2) $\lambda_y = -0.052$, and (e-2) $\lambda_y = -0.003$.

the attractor has a positive value of λ_y and is thus classified as a chaotic attractor. Conversely, the attractors in (b-2), (c-2), (d-2), and (e-2) have a negative Lyapunov exponents λ_y , and the phase sensitivity function $\Gamma(t)$ for these attractors is shown in Figure 5(a). In Figure 5(a), it can be seen that $\Gamma(t)$ for the attractor in (e-2) converges to a constant

value for large t . In contrast, $\Gamma(t)$ values for the attractors in (b-2), (c-2), and (d-2) do not converge to constant values; instead they increase with t algebraically. Therefore, it can be concluded that $\mu = 0$ for the attractor shown in (a-2), and $\mu > 0$ for those in (b-2), (c-2), and (d-2). As a consequence, the attractors shown in Figure 3 are classified as follows: (a-2) shows a chaotic attractor; (b-2), (c-2), and (d-2) show SNAs; and (e-2) shows a torus.

Next, for Case 2, shown in Figure 4, the attractor in (c-2) has a positive λ_y and is therefore a chaotic attractor. On the other hand, the attractors shown in (a-2), (b-2), (d-2), and (e-2) have negative λ_y . From Figure 5, it can be seen that the attractors shown in (a-2) and (b-2) of Figure 4 are tori, (c-2) shows a chaotic attractor, and (d-2) and (e-2) show SNAs.

In addition, for Case 1, it can be seen from Figure 3 that the torus becomes an SNA, and the SNA changes to chaos as the value of b is increased. In contrast, in Case 2 shown in Figure 4, the torus changes into an SNA via chaotic behavior. From these observations, it is concluded that the dynamical system given by (1)–(3) may also possess a variety of bifurcation structures.

5. Conclusions

An external quasiperiodic signal has been applied to a chaotic neuron circuit. In general, it is difficult to obtain a precise value for the non-positive largest Lyapunov exponent from the experimentally obtained time series from the circuit. Therefore, a mathematical model of the circuit was constructed by using a spline interpolation of the nonlinear output function. It was then possible to analyze the attractors from the model instead of those from the experiments. By using the Lyapunov exponents and phase sensitivity exponents calculated from the surrogate mathematical model, the experimental results could be evaluated and, as a result, SNAs were found among the observed attractors. In addition, changes in the attractor type with changing amplitude of the external force suggests the possibility of a variety of bifurcation structures in the output behavior of the chaotic neuron circuit when driven by an external quasiperiodic signal.

Acknowledgments

This research is partially supported by the Aihara Innovative Mathematical Modelling Project, the Japan Society for the Promotion of Science (JSPS) through the “Funding Program for World-Leading Innovative R&D on Science and Technology (FIRST Program),” initiated by the Council for Science and Technology Policy (CSTP), and Kakuhhi (20300085).

References

[1] C. Grebogi, E. Ott, S. Pelikan, and J. A. Yorke, “Strange attractors that are not chaotic,” *Physica. D*, vol.13, pp.261–268, 1984.

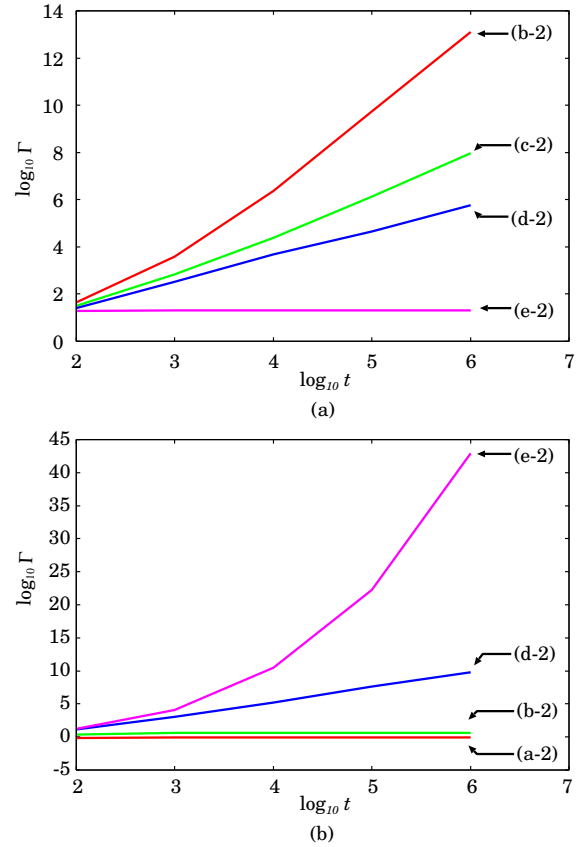


Figure 5: Log-log plots of Γ with respect to t for the attractors shown in (a) Figure 3, and (b) Figure 4.

- [2] T. Mitsui and Y. Aizawa, “Intermittency route to strange nonchaotic attractors in a non-skew-product map,” *Phys. Rev. E*, vol.81, 046210, 2010.
- [3] W. Lim and S. -Y. Kim, “Strange nonchaotic oscillations in the quasiperiodically-forced Hodgkin-Huxley neuron,” *J. Phys. A: Math. Theor.*, vol.42, 265103, 2009.
- [4] Z. Zhu and Z. Liu, “Strange nonchaotic attractors of chua’s circuit with quasiperiodic excitation,” *Int. J. Bifurcation and Chaos.*, vol.7, No. 1, pp.227–238, 1997.
- [5] K. Thamilmaran, D. V. Senthilkumar, A. Venkatesan, and M. Lakshmanan, “Experimental realization of strange nonchaotic attractors in a quasiperiodically forced electronic circuit,” *Phys. Rev. E*, vol.74, 036205, 2006.
- [6] A. Prasad, S. S. Negi, and R. Ramaswamy, “Strange nonchaotic attractors,” *Int. J. Bifurcation Chaos Appl. Sci. Eng.*, vol.11, pp.291–391, 2001.
- [7] K. Aihara, T. Takabe, and M. Toyoda, “Chaotic neural networks,” *Phys. Lett. A*, vol.146, pp.333–340, 1990.
- [8] Y. Horio, O. Yamamoto, and K. Aihara, “Neuron-synapse IC chip-set for large-scale chaotic neural networks,” *IEEE Trans. Neural Networks*, vol.14, No. 5, pp.1393–1404, 2003.
- [9] A. S. Pikovsky and U. Fedel, “Characterizing strange nonchaotic attractors,” *Chaos*, vol.5, pp.253–260, 1995.